








# Plagued by a cryptic clock

## Insight and issues from the global phylogeny of *Y. pestis*.

This manuscript ([permalink](#)) was automatically generated from [ktmeaton/obsidian-public@d4a820fb](#) on September 13, 2021.

### Authors

---

- **Katherine Eaton**  [0000-0001-6862-7756](#)  
McMaster Ancient DNA Center; Department of Anthropology, McMaster University
- **Leo Featherstone**  [0000-0002-8878-1758](#)  
The Peter Doherty Institute For Infection and Immunity , University of Melbourne
- **Sebastian Duchene**  [0000-0002-2863-0907](#)  
The Peter Doherty Institute For Infection and Immunity , University of Melbourne
- **Ann Carmichael**  
Indiana University Bloomington
- **Nükhet Varlık**  [0000-0001-6870-5945](#)  
University of South Carolina
- **Brian Golding**  [0000-0002-7575-0282](#)  
Department of Biology, McMaster University
- **Eddie Holmes**  [0000-0001-9596-3552](#)  
University of Sydney
- **Hendrik Poinar**  [0000-0002-0314-4160](#)  
McMaster Ancient DNA Center; Department of Anthropology, McMaster University

# Introduction

---

- Plague has a powerful and lasting legacy. Tremendous societal change.
- Humanity has been visited by many waves of plague pandemics
- Bronze Age to current epidemics, has visited every continent, and remains endemic in x of those.

# Results and Discussion

---

## Population Structure

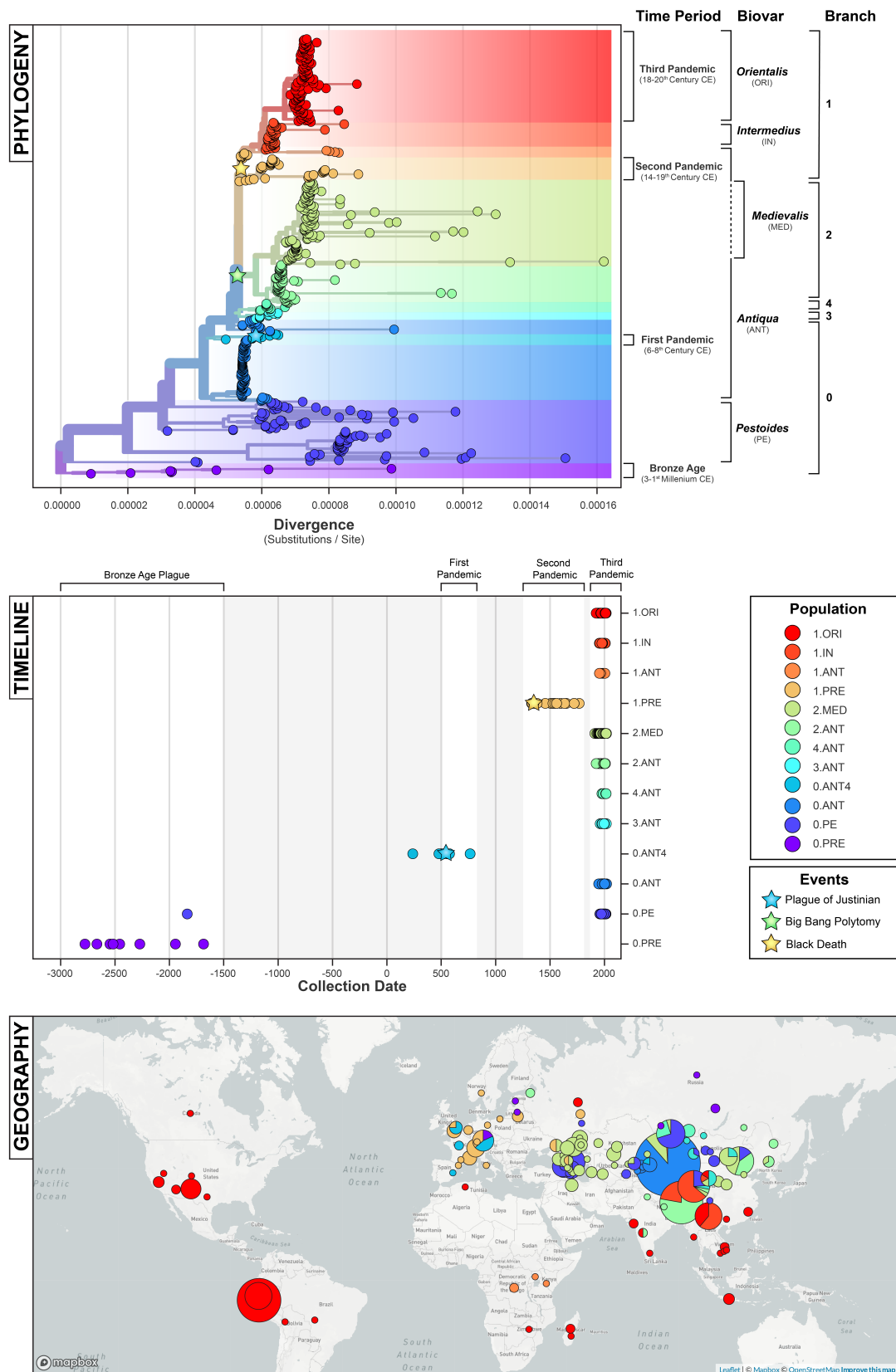
A critical step in reconstructing the evolutionary history of an organism is exploring the degree of population or genetic structure [1]. This structure develops as a populations subdivide and diversify in isolation, producing a pattern of lower diversity within groups and higher diversity between them. This knowledge can then be used to add nuance to phylogenetic analyses and interpretations, by explicitly modeling these unique evolutionary histories. However, there is little consensus concerning the genetic structure of *Y. pestis* on a global scale, and it was recently proposed [2] that our understanding of population structure should be revised according to the latest genomic data.

We therefore began by estimating a maximum-likelihood phylogeny, using 601 global isolates including 540 modern (89.9%) and 61 ancient (10.1%) strains. In addition, two genomes of the outgroup taxa *Yersinia pseudotuberculosis* were included to root the tree. The alignment consisted of 10,249 variant positions exclusive to *Y. pestis*, with 3,844 sites shared by at least two strains. Following phylogenetic estimation, we pruned the outgroup taxa from the tree to more closely examine the genetic diversity of *Y. pestis*.

In Figure 1, we contextualize the global phylogeny using three widely-used nomenclature systems: the major branches, metabolic biovars, and historical time periods. In the following section, we compare and critique each system, identify any incongruent divisions and uncertainty, and explore an integrative approach for spatiotemporal analyses.

## Biovar

The oldest system to date is the biovar nomenclature, which uses metabolic differences to define population structure. *Y. pestis* can be categorized into four classical biovars: *antiqua* (ANT), *medievalis* (MED), *orientalis* (ORI), and *microtus/pestoides* (PE) [3,4]. Non-classical biovars have also been introduced, such as the *intermedium* biovar (IN), which reflects a transitional state from *antiqua* to *orientalis* [5]. The biovar system is simple in application, as it largely focuses on two traits: the ability to ferment glycerol and reduce nitrate [4]. However, this simplicity is offset by the growing recognition of regional inconsistencies in metabolic profiles [2], which weakens its broader applicability. This is further exacerbated by the sequencing of non-viable, 'extinct' *Y. pestis*, for which metabolic sub-typing is impossible [6]. Researchers have responded to this uncertainty in a variety of ways, by creating pseudo-biovars (PRE) [7] or extrapolating existing ones [8]. Other still have foregone the *biovar* nomenclature altogether in favor of locally-developed taxonomies [2]. Despite extensive research, it remains unclear which metabolic traits, if any, can be used to classify *Y. pestis* into distinct populations at a global scale.



Powered by Nextstrain (Hadfield et al Bioinformatics)

**Figure 1:** The phylogenetic, temporal, and geographic distribution of *Yersinia pestis* genomes. Top: The maximum-likelihood phylogeny. Middle: The timeline of collection dates. Bottom: The global geographic distribution.

## Major Branch

In contrast to the biovar nomenclature which emphasizes phenotype, the major branch nomenclature focuses on the evolutionary relationships between strains. This system divides the global phylogeny of *Y. pestis* into populations according to their relative position to the “Big Bang” polytomy [9]. All lineages that diverged prior to this polytomy are grouped into Branch 0 and those diverging after form Branches 1-4. Because this multifurcation plays such a central role in this system, there is great interest in estimating its timing and geographic origins [10]. However, the epidemiological significance of the “Big Bang” polytomy remains unclear, as no definitive phenotype has been identified that correlates with the observed branching pattern [???]. While the major branch system excels at reconstructing the evolutionary relationships between candidate populations, it struggles to connect these relationships to other biological changes.

## Time Period

As previously mentioned, the sequencing of ancient *Y. pestis* poses a problem for classification, as direct metabolic testing is impossible for these non-viable samples. Ancient DNA researchers thus use an alternative strategy, by incorporating contextual evidence such as the collection date or associated time period. The known genetic diversity of *Y. pestis* has been most commonly divided into four time periods: the Bronze Age (3rd - 1st millennium BCE) [7], the First Pandemic, (6th - 8th century CE) [8], the Second Pandemic (14th - 18th century CE) [11], and the Third Pandemic (19th - 20th century CE) [9].

The key strength of this nomenclature is that it provides an excellent foundation for interdisciplinary discourse. However, this system runs the risk of grouping unrelated populations, as contemporaneous strains have been observed to have distinct evolutionary histories [12]. Furthermore, there is growing awareness of the temporal overlap of the Second and the Third Pandemics. Previously, the temporal extents of these events were mutually exclusive, dating from the 14th to 18th century, and the late 19th to mid-20th century respectively [13]. Recent historical scholarship has contested this claim, and demonstrated that these constraints are a product of a Eurocentric view of plague [14]. The Second Pandemic is now recognized to have extended into at least the 19th Century [15,16] and the Third Pandemic is hypothesized to have begun as early as the 18th century in southern China [17]. Unfortunately, this period of overlap remains genomically unsampled, thus it is unclear where exactly to draw a genetic distinction, if it even exists, between these pandemic events.

Another limitation of this system is that several populations are curiously excluded from the time period nomenclature which emphasizes historically documented pandemics. For example, Branch 2 populations emerged at the same time as, but separate from, the Second Pandemic and have been associated with high mortality epidemics [18]. In particular, the *medievalis* population (2.MED) has spread throughout Asia (Figure 1) and was observed to have the fastest spread velocity of any *Y. pestis* lineage [17]. Given this epidemiological significance, it is surprising that Branch 2 populations have been largely overlooked in the pandemic taxonomy of *Y. pestis*. As ancient DNA sampling strategies expand in geographic scope, it will be important to consider how to adapt and expand the historical period nomenclature to encompass this new diversity.

## Uncertainty

In light of this uncertainty and inconsistencies, no classification system comprehensively represents the global population structure of *Y. pestis*. Instead, integrative approaches have been previously used in large comparative studies of *Y. pestis* [9,19]. We therefore take the intersection of the three

taxonomic systems discussed previously, to define 12 populations for statistical analysis (Figure [1](#) Legend). In the following sections, we highlight the novel insight and issues that arise when this population structure is incorporated into spatiotemporal analysis.

# Phylogenetics

A long-standing line of inquiry in plague phylogenetics has been estimating evolutionary rates in order to date internal nodes. Key areas of the phylogeny that have been intensively researched are the first emergence of *Y. pestis* in human populations [7], the “Big Bang” polytomy [10], and the onset of past pandemics [6,8,9]. Recent technological advancements, such as ancient DNA sequencing and new molecular clock methods, have enabled researchers to reach further back in time with increasingly complex models. But despite this intensive interest and methodological advancement, *Y. pestis* remains notoriously difficult to model using a molecular clock approach.

This difficulty can largely be attributed to the substantial rate variation that has been documented across the phylogeny of *Y. pestis* [9,11]. As a result, considerable debate has emerged over whether *Y. pestis* has absolutely no temporal signal [8], or if populations have such distinct rates that a species-wide signal is obscured [11,20]. This uncertainty has produced radically different temporal models between studies, with node dates shifted by as much as several millennia [7,9]. Thus a comprehensive understanding of plague’s molecular clock, or lack thereof, is necessary before we can begin to untangle when and where this disease appeared in the past.

## Rate Variation

In light of this evolutionary debate, we began our temporal analysis by exploring the extent of rate variation present in our updated genomic dataset, which is notably larger and more diverse than those used in previous studies [11]. Given this expanded diversity, it is unsurprising that a root-to-tip regression on collection date reproduces the finding that substitution rates in *Y. pestis* are poorly represented by a simple linear model or “strict clock” (Figure 2). While there is a statistically significant relationship between collection date and genetic distance to the root ( $P\text{-value}=4.959 \times 10^{-13}$ ), an extremely low coefficient of determination ( $R^2=0.09$ ) indicates there is tremendous variation that is not accounted for.

Thus far, the hypotheses proposed to explain this variation have primarily focused on ecological processes, such as the cycling between endemic and epidemic phases [9] and geographic expansions over large distances [11]. However, we argue that several methodological factors must first be taken into account, before investigating more complex ecological factors such as host and landscape.

## Time Dependency

One striking methodological factor is the time dependency of molecular rates. In Figure 2, we show how rate variation in *Yersinia pestis* correlates with the sampling time frame, in which populations sampled over several millennia (Bronze Age) have less variation than those sampled over multiple centuries (Second Pandemic) or decades (*medievalis*). This correlation is a well-known and widely-documented phenomenon in many organisms [21] and occurs due to two conflicting signals: a slower, long-term substitution rate combined with a higher, short-term mutation rate.

Separating out these signals can be extremely challenging and failure to do so can have significant consequences when estimating and interpreting a molecular clock. Of particular concern for epidemiological investigations is the risk of artificially inflating the substitution rate due to transient mutations, which will lead to underestimating internal node dates. With regards to plague genomics, this may result in incorrect molecular dates linked to key historical events, such as the emergence of pandemic populations. Because of this risk, we first evaluate the presence of spurious mutations in our dataset before attempting to estimate a molecular clock model.

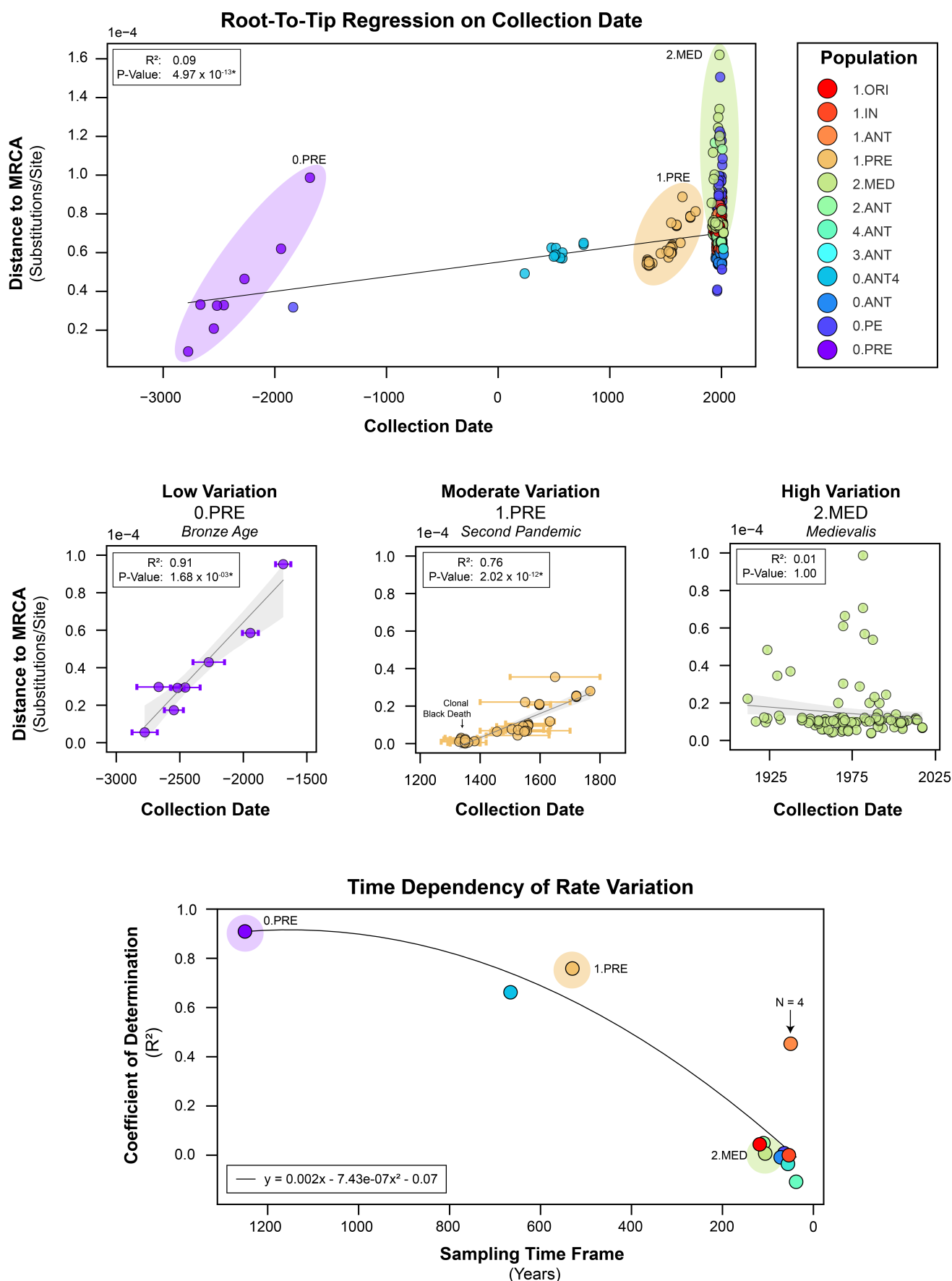


**Figure 2:** Rate variation in *Yersinia pestis* as observed through a regression of root-to-tip distances on collection date. Top: A species-wide model using all genomes from the maximum-likelihood phylogeny. Middle: Population-specific models based on extracted subtrees from the phylogeny. Bottom: The time-dependency of population-specific rate variation on the sampling time frame.



## Slow, Long-Term Substitution Rate

*Y. pestis* is particularly susceptible to the time-dependency of molecular rates, as it has one of the slowest substitution rates observed among bacterial pathogens [20]. The substitution rate of *Y. pestis* has previously been estimated to range from  $1 \times 10^{-8}$  to  $2 \times 10^{-8}$  substitutions/site/year [9,11], or 1 substitution every 10 to 25 years. In application, this means that *Y. pestis* lineages often cannot be differentiated until multiple decades have passed, a concept generally referred to as the phylodynamic threshold [22].

A historical example of this can be seen during the Second Pandemic, where isolates dated to the medieval Black Death (1348-1353) are nearly indistinguishable clones (Figure 2). A modern example is the *medievalis* population, where the youngest samples (2010s) have diverged little compared to those from a century prior (1910s). This highlights a significant limitation and cautionary note for *Y. pestis* phylogenetics, as comparisons over short time scales (10 to 100 years) may have limited resolving power. Furthermore, the little phylogenetic signal that accumulates in the population may be easily obscured or biased by spurious mutations in a single sample.

## High, Short Term Mutation Rate

The *medievalis* population is an extreme example of mutational bias, as several samples collected between 1970 and 1980 are exceptionally divergent (Figure 2). This short-term diversity is largely due to mutations observed in only a single isolate, which manifest as long terminal branches in the maximum-likelihood phylogeny (Figure 1, Figure 4). The presence of transient mutations, or long branches, is not isolated to the *medievalis* population and also strongly impacts the *pestoides* (0.PE), *intermedium* (1.IN), and *orientalis* (1.ORI) populations (Figure 3). Given the extensive presence of these apparent outliers, inclusion or exclusion of these samples may have profound impacts on spatiotemporal analyses. Specifically, these populations may appear to have more rate acceleration events, a faster rate of spread, and unexpectedly young node dates.

## Bayesian Evaluation of Temporal Signal (BETS)

As the root-to-tip regression revealed poor support for a strict clock (Figure 2), our next step was to model the observed rate variation using a relaxed clock. To investigate the degree of temporal structure in *Y. pestis*, we performed a Bayesian evaluation of temporal signal (BETS) test [23]. In brief, this method compares the likelihoods of two different phylogenetic models, one where the true collection dates are used and the other where all collection dates are assumed to be contemporaneous. A comparison of the model likelihoods, or Bayes factors, is then used to assess the degree of temporal signal in the dataset. We performed this test using both strict and relaxed clocks (uncorrelated lognormal), and compared their performance in species-wide and population-specific models (Figure 3).

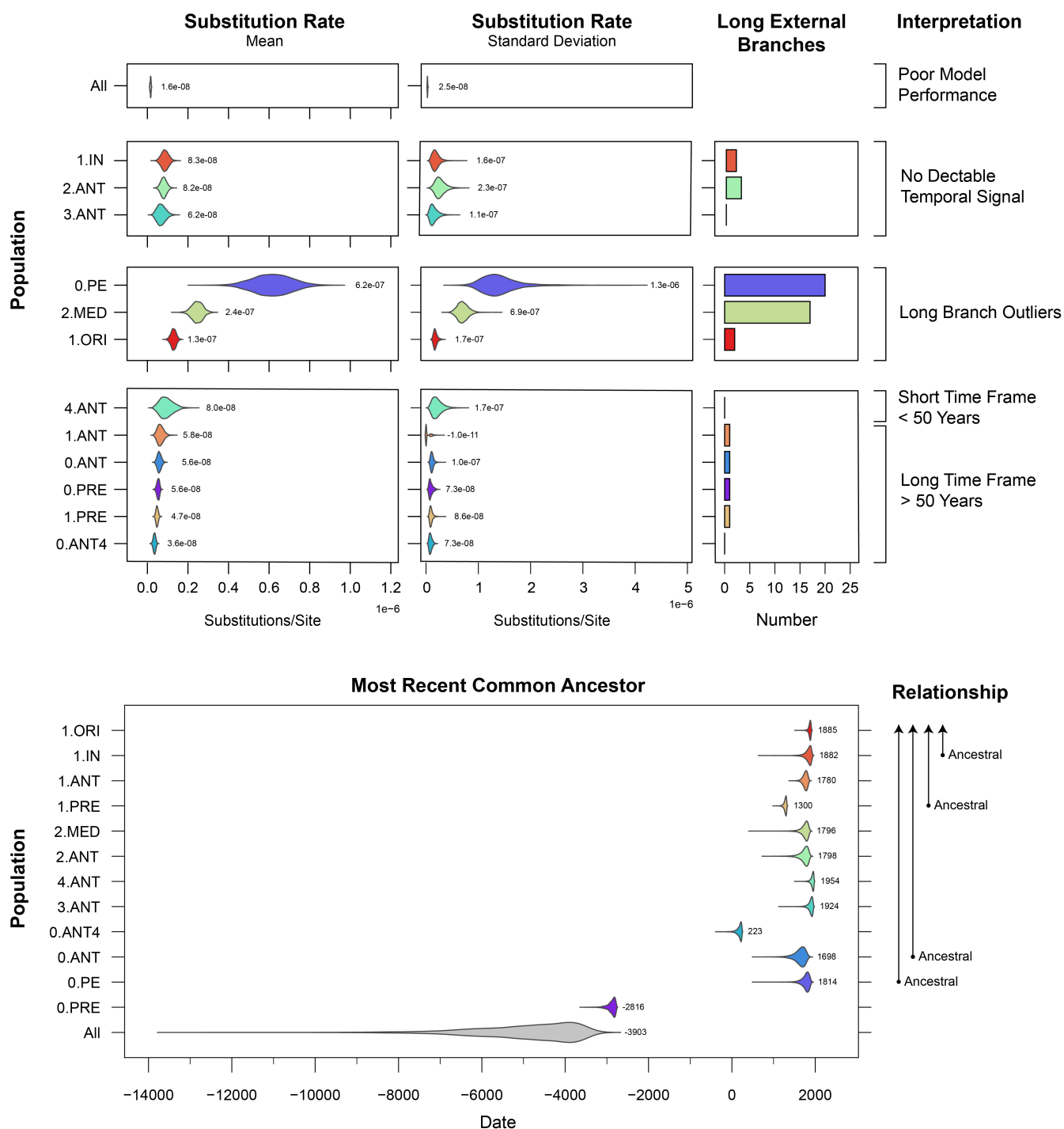


**Figure 3:** The estimated substitution rates and dates of the most recent common ancestors (MRCA). Each distribution is annotated with the peak value.

## Poor Performance of a Species Clock

The BETS test was inconclusive when attempting to estimate a single clock for all *Y. pestis* populations combined. The Bayesian analysis exhibited poor sampling of the clock parameters, for both a strict and relaxed clock, even when attempting to reduce sources of variation such as decreasing the number of genomes, using fixed tip dates, and fixing the tree topology. The clock model estimated with this approach had the lowest mean substitution rate ( $1.6 \times 10^{-8}$ ) and the least variation ( $2.5 \times 10^{-8}$ ) observed in this study. Overall, this poor performance is consistent with previous analyses [8] where robust estimates of model parameters could not be estimated, thus leading to the conclusion that *Y. pestis* lacks temporal signal. However, as other studies have suggested data composition is a strong determinant of temporal signal [20] we then repeated the BETS test by modeling each of the 12 populations of *Y. pestis* in isolation.

## Incongruent Population Clocks

In contrast to the species-wide model, separating the genomic dataset by population dramatically stabilized the Bayesian analysis. Temporal signal was detected in 9 out of 12 populations (Table 1) and all clock model parameters were well-sampled with effective sample sizes (ESS) greater than 200. However, we observed that improvements in model performance did not necessarily lead to improvements in model accuracy.

Without the calibrating influence of pre-modern *Y. pestis*, the modern populations were frequently estimated to have dates that violated the ancestor-descendant relationships present in the maximum-likelihood phylogeny (Figure 3). For example, the most recent common ancestor (MRCA) of the *pestoides* biovar (0.PE) falls ancestral to the First Pandemic population (0.ANT4) and thus must pre-date the 6<sup>th</sup> century. Instead, the MRCA of the *pestoides* population was dated to approximately 1814. Similarly, the *intermedium* (1.IN) population falls ancestral to the Third Pandemic population (1.ORI) and yet their root node dates are contemporaneous (1882 and 1885 respectively). Thus despite having measurable temporal signal and objectively good model performance according to Bayesian criteria, several population clocks were incongruent.

## Long Branch Outliers

To some extent, these inconsistencies can be explained by the presence of transient mutations. The populations with the fastest rates and greatest variation also had the highest number of long external branches, and include *pestoides* (0.PE), *medievalis* (2.MED) and *orientalis* (1.ORI). As discussed previously, a higher prevalence of transient mutations can lead to artificially inflated substitution rates and estimated node dates that are too young. By this logic, we caution that node dates associated with these populations should be treated as highly suspect, and likely underestimates of the true divergence dates.

█ Extrapolations outside the sampling time frame are very fragile!

## Sampling Time Frame

The time-dependency of molecular rates

For example, all clock model parameters appeared to be robust according to objective Bayesian criteria, such as the degree of chain mixing and ESS scores. However, ... had dates for the most recent

common ancestor (MRCA) that violated the ancestor-descendant relationships present in the maximum-likelihood phylogeny. For example, the root of the *pestoides* biovar (0.PE) is ancestral to the First Pandemic population (0.ANT4) and thus must pre-date the 6<sup>th</sup> century. Instead, the MRCA of the *pestoides* population was dated to approximately 1814. Similarly, the 0.ANT population is also ancestral to the First Pandemic, but has an estimated root date of 1698. Finally, the *intermedium* (1.IN) population is ancestral to the Third Pandemic population (1.ORI biovar and yet their root node dates are contemporaneous (1882 and 1885 respectively).

To some extent, these inconsistencies can be explained by the presence of transient mutations. The populations with the five highest mean substitution rates and standard deviations also have the five highest number of long, external branches (0.PE, 2.MED, 2.ANT, 1.ORI, 1.IN). As discussed previously, a higher prevalence of transient mutations can lead to artificially inflated substitution rates and estimated node dates that are too young. By this logic, we caution that node dates associated with these populations should be treated as highly suspect, and likely underestimates of the true divergence dates.

- Accurate clock model estimates for *Y. pestis* require long-term heterochronous sampling. On the order of multiple centuries. More exact estimates of the phylodynamic threshold could be

## Rate Overestimation

The first finding is that several populations have anomalously high substitution rates, namely the *pestoides* (0.PE) and *medievalis* (2.MED) biovars. As previously mentioned, this pattern may be explained by a high number of transient mutations. Indeed, the five populations with the highest number of long terminal branches (0.PE, 2.MED, 1.ORI, 1.IN, 2.ANT), have the five highest mean rates and standard deviations. Furthermore, two of these populations (1.IN, 2.ANT) have no detectable temporal signal. As discussed previously, if these inflated rates are due to spurious mutations rather than fixed substitutions, internal node dates will be unexpectedly young. Fortunately, this can be critiqued using the branching order of the maximum-likelihood phylogeny, as many of these populations are not monophyletic, and have ancestor-descendant relationships between them.

The most striking example of inconsistent node dating is the *pestoides* biovar (0.PE). The date of this population's root node, or most recent common ancestor (MRCA), was estimated at approximately 1814. However, this date is topologically inconsistent, as the root of the *pestoides* population falls ancestral to the Plague of Justinian (6<sup>th</sup> century) and thus must pre-date this event (Figure 1). Similarly, the *intermedium* (1.IN) population falls ancestral to the *orientalis* biovar (1.ORI) and yet their root node dates are contemporaneous (1882 and 1885 respectively). The remaining two possible outliers, 2.MED and 2.ANT, are monophyletic clades and thus have no descendant populations to serve as an upper bound. But we cautiously propose that the root dates of these two populations, 1796 and 1798 respectively, should be treated as highly suspect and likely an underestimate of the true divergence dates.

This means that 68% of the phylogeny (411/601 genomes) has unreliable clock estimates. So where does that leave us?

Without the calibrating influencing of ancient DNA samples or the larger phylogeny, the rates and dates associated with the *pestoides* biovar should be treated as highly suspect.

Should be very cautious trying to date inter-population nodes, ie. the Big Bang Polytoimy. Because we don't fully understand how the rate changes in between them.

## A New Global Rate

The second finding is that substitution rates in *Y. pestis* have been previously underestimated. The mean substitution rate we estimated from all populations combined, which was highly unstable, was  $1.6 \times 10^{-8}$ , which falls within published range of  $1$  to  $2 \times 10^{-8}$ . However, no *Y. pestis* population was observed to have a mean substitution rate this slow. Instead ranged from  $3.6 \times 10^{-8}$  during the First Pandemic (O.ANT4 to  $6.16 \times 10^{-7}$  in the *pestoides* biovar (O.PE). This study therefore reports the substitution rate of *Y. pestis* to be much higher than previously thought and more comparable to bacteria such as *Mycobacterium tuberculosis* [20].

As mentioned previously, inaccurate substitution rates have important consequences for node-dating. Specifically, underestimating the global rate leads to overestimating the age of the MRCA.

## Phylogeography

## Conclusions

---

# Methods

---



# References

---

1. **Did Our Species Evolve in Subdivided Populations across Africa, and Why Does It Matter?**  
Eleanor M. L. Scerri, Mark G. Thomas, Andrea Manica, Philipp Gunz, Jay T. Stock, Chris Stringer, Matt Grove, Huw S. Groucutt, Axel Timmermann, G. Philip Rightmire, ... Lounès Chikhi  
*Trends in Ecology & Evolution* (2018-08) <https://www.ncbi.nlm.nih.gov/pmc/articles/PMC6092560/>  
DOI: [10.1016/j.tree.2018.05.005](https://doi.org/10.1016/j.tree.2018.05.005) · PMID: [30007846](https://pubmed.ncbi.nlm.nih.gov/30007846/) · PMCID: [PMC6092560](https://pubmed.ncbi.nlm.nih.gov/PMC6092560/)
2. **Phylogeny and classification of *Yersinia pestis* through the lens of strains From the plague foci of Commonwealth of Independent States**  
Vladimir V. Kutyrev, Galina A. Eroshenko, Vladimir L. Motin, Nikita Y. Nosov, Jaroslav M. Krasnov, Lyubov M. Kukleva, Konstantin A. Nikiforov, Zhanna V. Al'khova, Eugene G. Oglodin, Natalia P. Guseva  
*Frontiers in Microbiology* (2018-05-25) <https://www.frontiersin.org/article/10.3389/fmicb.2018.01106/full>  
DOI: [10.3389/fmicb.2018.01106](https://doi.org/10.3389/fmicb.2018.01106)
3. **Variétés de l'espèce *Pasteurella pestis***  
R. Devignat  
*Bulletin of the World Health Organization* (1951) <https://www.ncbi.nlm.nih.gov/pmc/articles/PMC2554099/>  
PMID: [14859080](https://pubmed.ncbi.nlm.nih.gov/14859080/) · PMCID: [PMC2554099](https://pubmed.ncbi.nlm.nih.gov/PMC2554099/)
4. **Comparative and evolutionary genomics of *Yersinia pestis***  
Dongsheng Zhou, Yanping Han, Yajun Song, Peitang Huang, Ruifu Yang  
*Microbes and Infection* (2004-11-01) <http://www.sciencedirect.com/science/article/pii/S1286457904002357>  
DOI: [10.1016/j.micinf.2004.08.002](https://doi.org/10.1016/j.micinf.2004.08.002)
5. **Genotyping and Phylogenetic Analysis of *Yersinia pestis* by MLVA: Insights into the Worldwide Expansion of Central Asia Plague Foci**  
Yanjun Li, Yujun Cui, Yolande Hauck, Mikhail E. Platonov, Erhei Dai, Yajun Song, Zhaobiao Guo, Christine Pourcel, Svetlana V. Dentovskaya, Andrey P. Anisimov, ... Gilles Vergnaud  
*PLOS ONE* (2009-06-22) <https://journals.plos.org/plosone/article?id=10.1371/journal.pone.0006000>  
DOI: [10.1371/journal.pone.0006000](https://doi.org/10.1371/journal.pone.0006000)
6. **A draft genome of *Yersinia pestis* from victims of the Black Death**  
Kirsten I. Bos, Verena J. Schuenemann, G. Brian Golding, Hernán A. Burbano, Nicholas Waglechner, Brian K. Coombes, Joseph B. McPhee, Sharon N. DeWitte, Matthias Meyer, Sarah Schmedes, ... Johannes Krause  
*Nature* (2011-10) <http://www.nature.com/articles/nature10549>  
DOI: [10.1038/nature10549](https://doi.org/10.1038/nature10549)
7. **Early Divergent Strains of *Yersinia pestis* in Eurasia 5,000 Years Ago**  
Simon Rasmussen, Morten Erik Allentoft, Kasper Nielsen, Ludovic Orlando, Martin Sikora, Karl-Göran Sjögren, Anders Gorm Pedersen, Mikkel Schubert, Alex Van Dam, Christian Mollin Outzen Kapel, ... Eske Willerslev  
*Cell* (2015-10-22) <https://www.ncbi.nlm.nih.gov/pmc/articles/PMC4644222/>  
DOI: [10.1016/j.cell.2015.10.009](https://doi.org/10.1016/j.cell.2015.10.009) · PMID: [26496604](https://pubmed.ncbi.nlm.nih.gov/26496604/) · PMCID: [PMC4644222](https://pubmed.ncbi.nlm.nih.gov/PMC4644222/)

8. ***Yersinia pestis* and the Plague of Justinian 541–543 AD: a genomic analysis**

David M Wagner, Jennifer Klunk, Michaela Harbeck, Alison Devault, Nicholas Waglechner, Jason W Sahl, Jacob Enk, Dawn N Birdsell, Melanie Kuch, Candice Lumibao, ... Hendrik Poinar  
*The Lancet Infectious Diseases* (2014-04) <https://linkinghub.elsevier.com/retrieve/pii/S1473309913703232>  
DOI: [10.1016/s1473-3099\(13\)70323-2](https://doi.org/10.1016/s1473-3099(13)70323-2)

9. **Historical variations in mutation rate in an epidemic pathogen, *Yersinia pestis***

Y. Cui, C. Yu, Y. Yan, D. Li, Y. Li, T. Jombart, L. A. Weinert, Z. Wang, Z. Guo, L. Xu, ... R. Yang  
*Proceedings of the National Academy of Sciences* (2013-01-08) <http://www.pnas.org/cgi/doi/10.1073/pnas.1205750110>  
DOI: [10.1073/pnas.1205750110](https://doi.org/10.1073/pnas.1205750110)

10. **How a microbe becomes a pandemic: a new story of the Black Death**

Monica H. Green  
*The Lancet Microbe* (2020-12-01) [https://www.thelancet.com/journals/lanmic/article/PIIS2666-5247\(20\)30176-2/abstract](https://www.thelancet.com/journals/lanmic/article/PIIS2666-5247(20)30176-2/abstract)  
DOI: [10.1016/s2666-5247\(20\)30176-2](https://doi.org/10.1016/s2666-5247(20)30176-2)

11. **Phylogeography of the second plague pandemic revealed through analysis of historical *Yersinia pestis* genomes**

Maria A. Spyrou, Marcel Keller, Rezeda I. Tukhbatova, Christiana L. Scheib, Elizabeth A. Nelson, Aida Andrades Valtueña, Gunnar U. Neumann, Don Walker, Amelie Alterauge, Niamh Carty, ... Johannes Krause  
*Nature Communications* (2019-10-02) <https://www.nature.com/articles/s41467-019-12154-0>  
DOI: [10.1038/s41467-019-12154-0](https://doi.org/10.1038/s41467-019-12154-0)

12. **Analysis of 3800-year-old *Yersinia pestis* genomes suggests Bronze Age origin for bubonic plague**

Maria A. Spyrou, Rezeda I. Tukhbatova, Chuan-Chao Wang, Aida Andrades Valtueña, Aditya K. Lankapalli, Vitaly V. Kondrashin, Victor A. Tsybin, Aleksandr Khokhlov, Denise Kühnert, Alexander Herbig, ... Johannes Krause  
*Nature Communications* (2018-06-08) <https://www.nature.com/articles/s41467-018-04550-9>  
DOI: [10.1038/s41467-018-04550-9](https://doi.org/10.1038/s41467-018-04550-9)

13. **Natural history of plague: perspectives from more than a century of research**

Kenneth L. Gage, Michael Y. Kosoy  
*Annual Review of Entomology* (2005)  
DOI: [10.1146/annurev.ento.50.071803.130337](https://doi.org/10.1146/annurev.ento.50.071803.130337) · PMID: [15471529](https://pubmed.ncbi.nlm.nih.gov/15471529/)

14. **New Science and Old Sources: Why the Ottoman Experience of Plague Matters**

Nükheth Varlık  
*The Medieval Globe* (2014) <https://scholarworks.wmich.edu/tmg/vol1/iss1/9/>

15. **The Ottomans During the Global Crises of Cholera and Plague: The View from Iraq and the Gulf.**

Isacar A. Bolaños  
*International Journal of Middle East Studies* (2019-11) <http://www.cambridge.org/core/journals/international-journal-of-middle-east-studies/article/ottomans-during-the-global-crises-of-cholera->

[and-plague-the-view-from-iraq-and-the-gulf/82A6A0E7CF8BD2138FA230AE4189057E](https://doi.org/10.1017/s0020743819000667)

DOI: [10.1017/s0020743819000667](https://doi.org/10.1017/s0020743819000667)

**16. The plague that never left: restoring the Second Pandemic to Ottoman and Turkish history in the time of COVID-19**

Nükhet Varlık

*New Perspectives on Turkey* (2020-11) <https://www.cambridge.org/core/journals/new-perspectives-on-turkey/article/plague-that-never-left-restoring-the-second-pandemic-to-ottoman-and-turkish-history-in-the-time-of-covid19/AE81F48AD6FEB71C42AAA2115A0307A9>

DOI: [10.1017/npt.2020.27](https://doi.org/10.1017/npt.2020.27)

**17. Wet climate and transportation routes accelerate spread of human plague**

Lei Xu, Leif Chr. Stige, Kyrre Linné Kausrud, Tamara Ben Ari, Shuchun Wang, Xiye Fang, Boris V. Schmid, Qiyong Liu, Nils Chr. Stenseth, Zhibin Zhang

*Proceedings of the Royal Society B: Biological Sciences* (2014-04-07) <https://royalsocietypublishing.org/doi/10.1098/rspb.2013.3159>

DOI: [10.1098/rspb.2013.3159](https://doi.org/10.1098/rspb.2013.3159)

**18. Evolution and circulation of *Yersinia pestis* in the Northern Caspian and Northern Aral Sea regions in the 20th-21st centuries**

Galina A. Eroshenko, Nikolay V. Popov, Zhanna V. Al'khova, Lyubov M. Kukleva, Alina N. Balykova, Nadezhda S. Chervyakova, Ekaterina A. Naryshkina, Vladimir V. Kutyrev

*PLOS ONE* (2021-02-11) <https://journals.plos.org/plosone/article?id=10.1371/journal.pone.0244615>

DOI: [10.1371/journal.pone.0244615](https://doi.org/10.1371/journal.pone.0244615)

**19. *Yersinia pestis* genome sequencing identifies patterns of global phylogenetic diversity**

Giovanna Morelli, Yajun Song, Camila J. Mazzoni, Mark Eppinger, Philippe Roumagnac, David M. Wagner, Mirjam Feldkamp, Barica Kusecek, Amy J. Vogler, Yanjun Li, ... Mark Achtman

*Nature Genetics* (2010-12)

DOI: [10.1038/ng.705](https://doi.org/10.1038/ng.705) · PMID: [21037571](https://pubmed.ncbi.nlm.nih.gov/21037571/) · PMCID: [PMC2999892](https://pubmed.ncbi.nlm.nih.gov/PMC2999892/)

**20. Genome-scale rates of evolutionary change in bacteria**

Sebastian Duchêne, Kathryn E. Holt, François-Xavier Weill, Simon Le Hello, Jane Hawkey, David J. Edwards, Mathieu Fourment, Edward C. Holmes

*Microbial Genomics* (2016-11-30) <https://www.ncbi.nlm.nih.gov/pmc/articles/PMC5320706/>

DOI: [10.1099/mgen.0.000094](https://doi.org/10.1099/mgen.0.000094) · PMID: [28348834](https://pubmed.ncbi.nlm.nih.gov/28348834/) · PMCID: [PMC5320706](https://pubmed.ncbi.nlm.nih.gov/PMC5320706/)

**21. Time Dependency of Molecular Rate Estimates and Systematic Overestimation of Recent Divergence Times**

Simon Y. W. Ho, Matthew J. Phillips, Alan Cooper, Alexei J. Drummond

*Molecular Biology and Evolution* (2005-07-01) <https://doi.org/10.1093/molbev/msi145>

DOI: [10.1093/molbev/msi145](https://doi.org/10.1093/molbev/msi145)

**22. Temporal signal and the phylodynamic threshold of SARS-CoV-2**

Sebastian Duchene, Leo Featherstone, Melina Haritopoulou-Sinanidou, Andrew Rambaut, Philippe Lemey, Guy Baele

*Virus Evolution* (2020-07-01) <https://doi.org/10.1093/ve/veaa061>

DOI: [10.1093/ve/veaa061](https://doi.org/10.1093/ve/veaa061)

**23. Bayesian Evaluation of Temporal Signal in Measurably Evolving Populations**

Sebastian Duchene, Philippe Lemey, Tanja Stadler, Simon YW Ho, David A Duchene, Vijaykrishna

Dhanasekaran, Guy Baele

*Molecular Biology and Evolution* (2020-11-01) <https://doi.org/10.1093/molbev/msaa163>

DOI: [10.1093/molbev/msaa163](https://doi.org/10.1093/molbev/msaa163)

## Supplementary Information

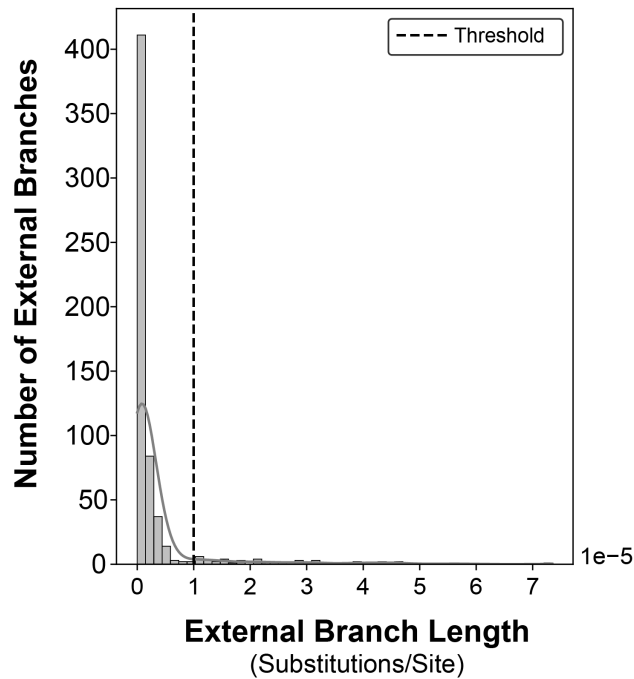


**Figure 4:** The distribution of external branch lengths across the maximum-likelihood phylogeny. The threshold to be considered a long external branch is set at 1e-5 substitutions/site.

**Table 1:** Model selection and log marginal likelihoods obtained from a Bayesian evaluation of temporal signal (BETS) test. \*0.PRE had temporal signal according to a strict clock, although the relaxed clock with no dates model had the highest likelihood.

| Population | N   | Time Span (Years) | Best Model    | Bayes Factor | Strict Clock No Dates | Strict Clock Dates | Relaxed Clock No Dates | Relaxed Clock Dates |
|------------|-----|-------------------|---------------|--------------|-----------------------|--------------------|------------------------|---------------------|
| 1.ORI      | 117 | 118               | Relaxed Clock | 36           | -5899691              | -5899661           | -5899601               | -5899566            |
| 1.IN       | 39  | 54                | –             | -10          | -5891399              | -5891403           | -5891344               | -5891355            |
| 1.ANT      | 4   | 50                | Relaxed Clock | 13           | -5882596              | -5882587           | -5882595               | -5882582            |
| 1.PRE      | 40  | 530               | Relaxed Clock | 44           | -5888140              | -5888130           | -5888082               | -5888038            |
| 2.MED      | 116 | 106               | Relaxed Clock | 4            | -5920837              | -5920733           | -5919662               | -5919658            |
| 2.ANT      | 54  | 110               | –             | -13          | -5892876              | -5892895           | -5892791               | -5892805            |
| 4.ANT      | 11  | 38                | Relaxed Clock | 4            | -5886031              | -5886034           | -5886026               | -5886022            |
| 3.ANT      | 11  | 56                | –             | -11          | -5887497              | -5887506           | -5887495               | -5887506            |
| 0.ANT4     | 12  | 666               | Relaxed Clock | 6            | -5889526              | -5889520           | -5889502               | -5889496            |
| 0.ANT      | 103 | 72                | Relaxed Clock | 13298        | -5896014              | -5896016           | -5895880               | -5882582            |

| Population | N  | Time Span<br>(Years) | Best<br>Model    | Bayes<br>Factor | Strict Clock<br>No Dates | Strict Clock<br>Dates | Relaxed Clock<br>No Dates | Relaxed<br>Clock Dates |
|------------|----|----------------------|------------------|-----------------|--------------------------|-----------------------|---------------------------|------------------------|
| 0.PE       | 85 | 64                   | Relaxed<br>Clock | 12              | -5945603                 | -5945574              | -5944627                  | -5944614               |
| 0.PRE      | 8  | 1250                 | Relaxed<br>Clock | 83*             | -5892926                 | -5892843              | -5892739                  | -5892741               |